Geochimica et Cosmochimica Acta 356 (2023) 105–115

Contents lists available at ScienceDirect

Geochimica et Cosmochimica Acta

journal homepage: www.elsevier.com/locate/gca

The importance of carbon to the formation and composition of silicates during mantle metasomatism

Michele Rinaldi [a,*], Sami Mikhail [a], Dimitri A. Sverjensky [b], Joanna Kalita [a]

[a] School of Earth and Environmental Sciences, University of St. Andrews, Queen's Terrace, St Andrews KY16 9TS, UK
[b] Department of Earth and Planetary Sciences, Johns Hopkins University, 301 Olin Hall 3400 N. Charles Street, Baltimore, MD 21218, USA

ARTICLE INFO

Associate editor: Rajdeep Dasgupta

Keywords:
Diamond inclusions
Fluid-rock metasomatism
Thermodynamic modelling

ABSTRACT

Mineral and fluid inclusions in mantle diamonds provide otherwise inaccessible information concerning the nature of mantle metasomatism and the role of fluids in the mass transfer of material through the Earth's interior. We explore the role of carbon concentration during fluid-rock metasomatism in generating the range of garnet and clinopyroxene compositions observed in diamonds from the sub-continental lithospheric mantle. We use the Deep Earth Water model to predict the results of metasomatism between silicic, carbonatitic and peridotitic fluids and common mantle rocks (peridotites, eclogites and pyroxenites) at 5 GPa, 1000 °C, across a range of redox conditions ($\log fO_2 = -2$ to -4 ΔFMQ), and a wide range of initial carbon concentrations in the metasomatic fluids. Our results show that the predicted compositions of metasomatic garnets and clinopyroxenes are controlled by the initial geochemistry of fluids and rocks, with subsequent mineral-specific geochemical evolution following definable reaction pathways. Model carbon-rich metasomatic fluids that can form diamond (initial C-content >5.00 molal) result in Mg-rich garnets and clinopyroxenes typical of peridotitic, eclogitic, and websteritic inclusions in diamonds. However, model carbon-poor metasomatic fluids that do not form diamond result in Mg-poor, Ca-rich garnets and clinopyroxenes. Such garnets and clinopyroxenes do nevertheless occur as inclusions in diamonds. In our models, the abundance of carbon in the fluids controls the behaviour of the bivalent ions through the formation of aqueous Mg-Ca-Fe-C complexes, which directly govern the composition of garnets and clinopyroxenes precipitated during the metasomatic processes. As the C-rich initial fluids can form the higher Mg-eclogitic, peridotitic, and websteritic inclusions in diamonds, these inclusions can be syngenetic (metasomatic) or possibly protogenetic. However, in our models, the relatively Mg-poor, Ca- and Fe-rich eclogitic garnet and clinopyroxene inclusions found in mantle diamonds formed from C-poor fluids that do not precipitate diamond. These inclusions most likely reflect a metasomatic event prior to being incorporated into their host diamonds, or they could represent protolith-based protogenetic geochemistry. Therefore, the paragenetic groups used to classify diamonds should not be considered a genetic classification, as the role of fluid geochemistry appears to be more important than the one played by host rock geochemistry.

1. Introduction

Experimental solubility data (Kessel et al., 2005a,b; Manning, 2013; Förster et al., 2019) and the cation concentration of fluid inclusions in diamonds (Navon et al., 1988; Weiss et al., 2015) show that aqueous fluids in equilibrium with mantle rocks contain all the rock-forming major and trace elements required to precipitate mantle-forming silicates (olivine, pyroxene, garnet). Therefore, the interaction(s) between rocks, fluids, and melts is Earth's most efficient mechanism for the mass transfer of material throughout the solid Earth. However, direct samples are scarce, with melt inclusions in silicates and fluid inclusions in diamonds being rare exceptions (Weiss et al., 2022). Owing to their robust and inert nature, mantle diamonds are extraordinary archives which provide otherwise inaccessible samples of solid, liquid, and gaseous material from Earth's interior. Diamonds have formed over more than 75% of Earth's history (Gurney et al., 2010; Koornneef et al., 2017; Gress et al., 2021), with most forming in the sub-continental lithospheric mantle (120–180 km; Stachel and Harris, 2008; Stachel et al., 2022). Therefore, the geochemistry of diamond inclusions preserves the most detailed and intact history of mantle metasomatism.

* Corresponding author.
E-mail addresses: mr267@st-andrews.ac.uk (M. Rinaldi), sm342@st-andrews.ac.uk (S. Mikhail), sver@jhu.edu (D.A. Sverjensky).

https://doi.org/10.1016/j.gca.2023.06.025
Received 23 September 2022; Accepted 26 June 2023
Available online 27 June 2023

Diamonds are metasomatic precipitates (Shirey et al., 2013; Miller et al., 2014). Their crystallisation can be driven by the transport of carbon-bearing material across adiabatic, isobaric, and isothermal geochemical gradients (Jacob et al., 2014; Luth and Stachel, 2014; Palyanov et al., 2015; Stagno et al., 2015; Sverjensky and Huang, 2015; Mikhail et al., 2021). The geochemistry of fluid inclusions in diamonds reveals four compositional groups: silicic, peridotitic, carbonatitic and saline (Navon et al., 1988; Izraeli et al., 2001; Tomlinson et al., 2006; Weiss et al., 2009, 2014, 2022; Timmerman et al., 2021) (Fig. 1a). The origin of diamond-forming fluids has been examined by experimental (e.g., Kessel et al., 2015; Bureau et al., 2018; Förster et al., 2019; Sonin et al., 2022; Meltzer and Kessel, 2022) and theoretical approaches (Huang and Sverjensky, 2020; Mikhail et al., 2021), alongside studies predicting the geochemistry of diamond-forming fluids which would be in equilibrium with solid silicate inclusions (e.g., Stachel and Harris, 2008; Aulbach et al., 2008; Mikhail et al., 2019a).

Compared with the geochemistry of the fluid inclusions in diamonds, the composition of mineral inclusions is more diverse (e.g., garnet compositions in Fig. 1b). Many mineral groups have been found as inclusions in diamonds, including sulfides, silicates, oxides, hydroxides, carbonates, and metallic phases (Stachel and Harris, 2008). However, one can subdivide these minerals into four groups: peridotitic, eclogitic, websteritic, and exotic metallic phases (Stachel et al., 2022). The inclusion classification schemes for both fluids and minerals are empirical; therefore, fluid and mineral classifications do not diagnostically reveal petrogenetic processes (Mikhail et al., 2021). In particular, the diversity of the petrological characteristics and the complexity of structural and textural elements leave the interpretation of the genetic relationships between diamonds and their mineral inclusions unclear. Mineral inclusions either reflect a pre-metasomatic heterogeneity in the host rock in the upper mantle (Pasqualetto et al., 2022) or the result of metasomatism coeval with diamond formation (Aulbach et al., 2002; Kiseeva et al., 2016; Mikhail et al., 2019b), or both options. Therefore, diamonds and their mineral inclusions can be either syngenetic (Harris, 1968; Mikhail et al., 2019b) or protogenetic (Nestola et al., 2017).

This contribution aims to investigate the geochemistry of silicates formed during isobaric (5 GPa) and isothermal (1000 °C) fluid-rock metasomatism benchmarked to the geochemistry of diamond inclusions. Specifically, we focused on garnets and clinopyroxenes because both are abundant in peridotitic, eclogitic, and websteritic paragenetic groups (Stachel et al., 2022).

2. Method

Conceptually, our computational thermodynamic model involves two steps. Firstly, a fluid is equilibrated with a rock (EQ3 in Fig. 2). Secondly, this fluid then migrates and interacts with a collection of mineral phases (a rock) at the same (fixed) pressure and temperature (EQ6 in Fig. 2). The fluid in step 2 is out of equilibrium with the rock, and this drives irreversible chemical reactions which produce new mineral phases while concurrent changes to the geochemistry of the fluid are reciprocated. Reaction path models such as these have been widely applied under near-surface conditions as well as temperatures and pressures corresponding to the crust (Helgeson, 1979; Sverjensky, 1984, 1987; McCollom and Shock, 1998; Shock and Canovas, 2010; Hao et al., 2016, 2017; Leong and Shock, 2020; Leong et al., 2021). However, models such as these have only recently been applied to fluid-rock interactions in the deep crust and upper mantle (e.g., Sverjensky and Huang, 2015; Huang and Sverjensky, 2020; Mikhail et al., 2021).

The range of initial carbon contents of the fluids used in the modelling can be related to different geological contexts, from the breakdown of hydrous wadsleyite into olivine + H_2O during the rising of a plume in the subcontinental lithosphere (low carbon fluids) to a fluid migrating from sediments carried downwards by the slab in a subduction zone (high carbon fluids; Poli, 2015; Tumiati et al., 2017; Yaxley et al., 2021). The P-T-X-fO_2 conditions used (P = 5 GPa, T = 1000 °C, logfO_2 = −2 to −4 ΔFMQ, where FMQ refers to Fayalite = Magnetite + Quartz redox buffer reaction) overlap with the average P-T-X-fO_2 conditions for lithospheric diamond inclusion formation, where the average inclusion entrapment temperature is 1155 ± 105 °C (n = 444) with corresponding pressures of 5.3 ± 0.8 GPa (n = 157) (Stachel and Harris, 2008; Stachel and Luth, 2015).

Fluid-rock interaction is complex and dynamic, where solid and fluid phases interact progressively. This results in irreversible geochemical evolution. Thermodynamic modelling of fluid-rock interaction above 0.5 GPa was precluded until the dielectric constant of water was constrained at ≤ 6 GPa (Sverjensky et al., 2014). Now, we can apply the Helgeson-Kirkham-Flowers (HKF) equations of state for aqueous speciation (Helgeson and Kirkham, 1974a,b, 1976; Helgeson et al., 1981; Tanger and Helgeson, 1988; Shock and Helgeson, 1988; Sverjensky et al., 1997) up to 6 GPa and 1200 °C (Pan et al., 2013; Facq et al., 2014; Sverjensky et al., 2014). As a result, it is now possible to model the fluid speciation of aqueous anions, metal complexes, and neutral species and their interaction with minerals across pressure and temperature conditions that resemble those from the surface and down to ca. 150 km inside planet Earth (Huang and Sverjensky, 2019, 2020; Mikhail et al., 2021).

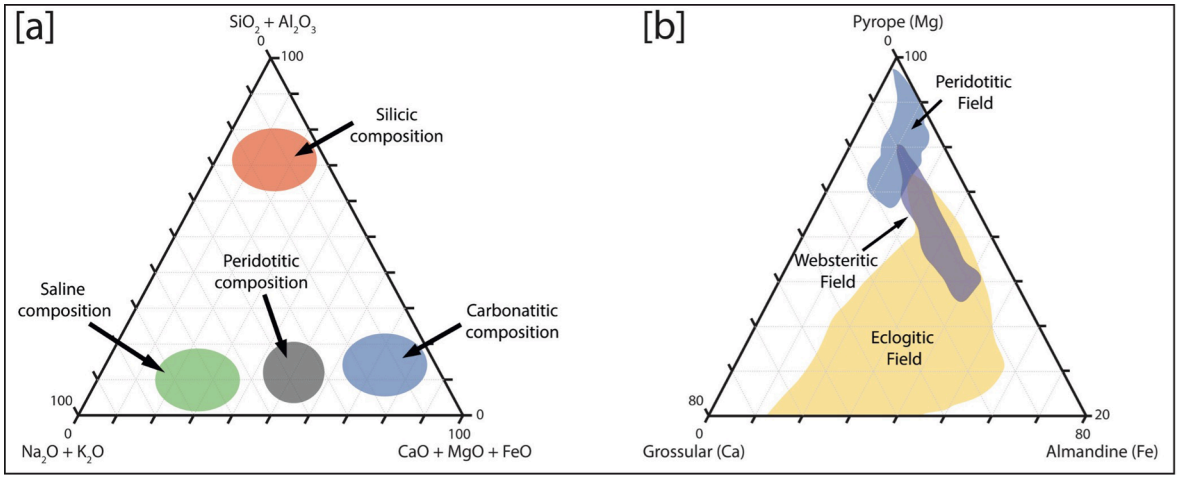

Fig. 1. Fluid and solid inclusions in diamonds: a) Compositional groups for fluid inclusions (Weiss et al., 2022); b) Mineral inclusions from numerous sources (see Methods). The poorly defined websteritic data cluster connects the peridotitic and eclogitic fields and represents different steps of a metasomatic evolution (Mikhail et al., 2021).

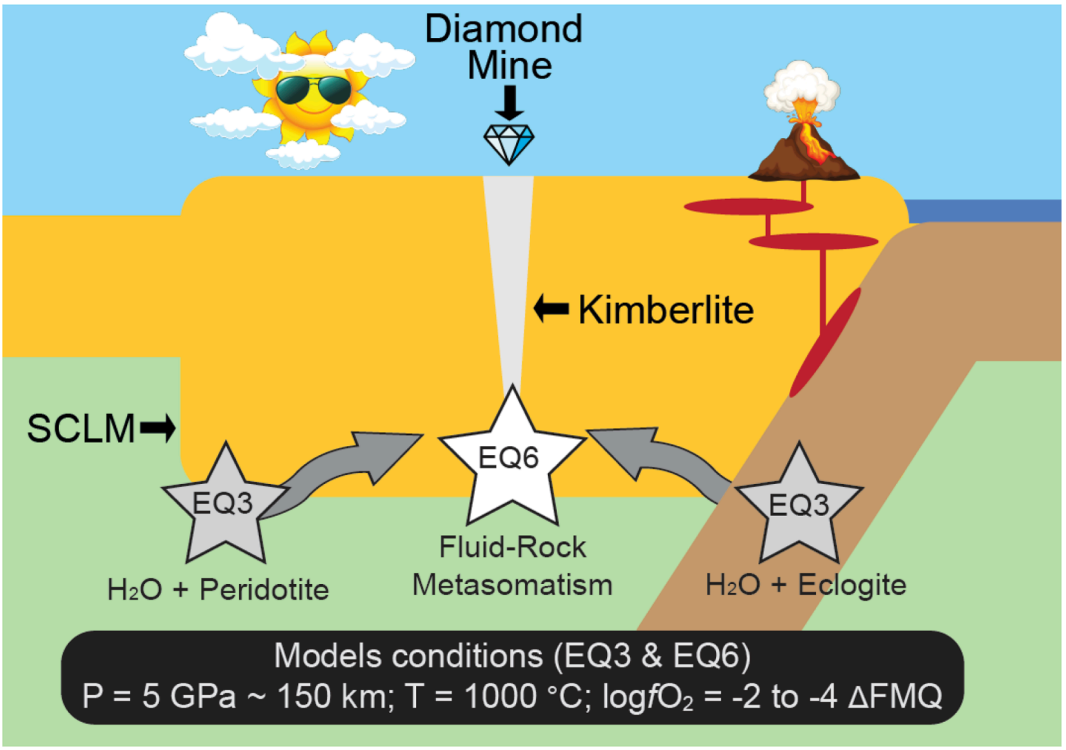

Fig. 2. Cartoon illustrating our conceptual modelling approach. We calculate the fluid composition for a given rock in equilibrium with water (EQ3), and then we compute the reaction of the resulting fluid with different lithologies (EQ6). Note that there are no spatial dimensions to our models. The fluid migration arrows shown above illustrate – contextually – the formation and migration of a mantle fluid that migrates into the cratonic lithosphere and reacts with rocks it encounters (i.e., simulating fluid metasomatism in the SCLM).

Technically, the modelling approach used in this study is a step-by-step dissolution of the reactant rock (Table 2) into the fluid (Table 1). Each unit of the reaction progress variable (ξ) corresponds to the destruction of 1.0 mole of each reactant mineral per 1.0 kg of H_2O in the initial fluid. As the reactants are progressively dissolved, the fluid geochemistry changes and the precipitation of new metasomatic minerals is triggered. The chemical composition of these new solid phases is in equilibrium with the fluid at each step of the modelling process. The process continues until the reactant rock is equilibrated with the fluid or the changes in the fluid geochemistry are no longer relevant.

The initial fluid compositions used are designed to mirror the compositions of fluid inclusions from diamonds described in the literature (i.e., silicic, peridotitic and carbonatitic; Weiss et al., 2009, 2022; Fig. 1a), which are equilibrated with a specific mantle rock (e.g., mineral assemblage; Table 1, Table S1–S3). The silicic fluid is based on an experimental calibration of aqueous fluid in equilibrium with a mafic eclogite (Kessel et al., 2015; later referred to as an eclogitic fluid), documented in Huang and Sverjensky (2020). For the peridotitic and carbonatitic fluids, we chose the peridotite and carbonated dunite used to model the fluid compositions to form Panda diamonds (Huang and Sverjensky, 2020), with garnet instead of spinel to match the higher temperature and pressure. We assumed an ideal site-mixing of garnet endmembers (pyrope, grossular, and almandine) and carbonates (calcite, magnesite, and siderite) and a non-ideal site-mixing of clinopyroxene endmembers (diopside, clinoenstatite, hedenbergite, and jadeite). The clinopyroxene solid solution was calibrated using natural samples of diamond inclusions as described previously (Huang and Sverjensky, 2020; Mikhail et al., 2021). To study the influence of carbon abundance and speciation on the geochemistry of silicate minerals, we ran models with a fixed initial amount of carbon at $\log fO_2 = -3$ ΔFMQ (from 0.00 to 1.00 molal; Table 1 and Table S3) for the eclogitic and peridotitic fluids. Due to the nature of the carbonatitic fluid, it was impossible to constrain the amount of carbon with a fixed value as it would have affected the entire mineral assemblage (e.g., carbonates).

Table 1
Composition (molality concentration [moles/kg H_2O]) of eclogitic, peridotitic, and carbonatitic fluids at 1000 °C, 5 GPa and $\log fO_2 = -3$ ΔFMQ.

Fluid	Type	Name	C	K	Na	Ca	Mg	Fe	Al	Si	Cl	pH
Eclogitic	Low-C fluids	E_0.00	0.00	0.00	1.05	0.68	0.01	0.06	1.16	11.57	0.00	4.49
		E_0.25	0.25	0.00	1.05	0.69	0.05	0.07	1.19	11.52	0.00	4.51
		E_0.50	0.50	0.00	1.04	0.70	0.09	0.09	1.21	11.46	0.00	4.52
		E_0.75	0.75	0.00	1.04	0.72	0.13	0.10	1.23	11.41	0.00	4.53
		E_1.00	1.00	0.00	1.04	0.73	0.16	0.12	1.25	11.36	0.00	4.54
	Diamond	E_dia	3.13	0.00	1.05	0.84	0.42	0.22	1.37	10.91	0.00	4.60
Peridotitic	Low-C fluids	P_0.00	0.00	2.45	2.00	0.78	0.21	1.71	0.10	2.36	8.00	4.51
		P_0.25	0.25	2.41	2.00	0.78	0.33	1.69	0.10	2.46	8.00	4.53
		P_0.50	0.50	2.37	2.00	0.79	0.46	1.67	0.10	2.56	8.00	4.54
		P_0.75	0.75	2.34	2.00	0.80	0.58	1.65	0.10	2.66	8.00	4.55
		P_1.00	1.00	2.30	2.00	0.81	0.70	1.63	0.11	2.78	8.00	4.56
	Diamond	P_dia	5.58	1.91	2.00	1.03	2.48	1.36	0.14	4.25	8.00	4.73
Carbonatitic	Diamond	C_dia	17.96	0.50	0.50	11.13	3.01	0.68	0.72	0.08	1.00	5.80

Table 2
Mineralogical and solid solution compositions of mantle rocks used during fluid-rock interaction.

Rock	Mineral composition (% in volume)
Lherzolite	51% ol ($Fo_{0.930}Fa_{0.067}$), 18% opx ($En_{0.938}Fe_{0.062}$), 26% cpx ($Di_{0.294}Hdn_{0.088}Ja_{0.015}En_{0.603}$), 5% grt ($Py_{0.733}Gr_{0.137}Alm_{0.130}$)
Harzburgite	71% ol ($Fo_{0.933}Fa_{0.067}$), 24% opx ($En_{0.938}Fe_{0.062}$), 5% grt ($Py_{0.733}Gr_{0.137}Alm_{0.130}$)
Dunite	83% ol ($Fo_{0.933}Fa_{0.067}$), 5% opx ($En_{0.938}Fe_{0.062}$), 7% cpx ($Di_{0.294}Hdn_{0.088}Ja_{0.015}En_{0.603}$), 5% grt ($Py_{0.733}Gr_{0.137}Alm_{0.130}$)
Eclogite type 1	41% cpx ($Di_{0.200}Hdn_{0.100}Ja_{0.700}En_{0.000}$), 26% grt ($Py_{0.600}Gr_{0.100}Alm_{0.300}$), 33% coe
Eclogite type 2	19% cpx ($Di_{0.200}Hdn_{0.100}Ja_{0.700}En_{0.000}$), 39% grt ($Py_{0.333}Gr_{0.334}Alm_{0.333}$), 42% coe
Eclogite type 3	25% cpx ($Di_{0.200}Hdn_{0.100}Ja_{0.700}En_{0.000}$), 75% grt ($Py_{0.200}Gr_{0.600}Alm_{0.200}$)
Websterite	5% ol ($Fo_{0.920}Fa_{0.080}$), 40% opx ($En_{0.750}Fe_{0.250}$), 50% cpx ($Di_{0.560}Hdn_{0.020}Ja_{0.020}En_{0.400}$), 5% grt ($Py_{0.500}Gr_{0.250}Alm_{0.250}$)
Orthopyroxenite	3% ol ($Fo_{0.890}Fa_{0.110}$), 92% opx ($En_{0.900}Fe_{0.100}$), 5% grt ($Py_{0.700}Gr_{0.100}Alm_{0.200}$)
Clinopyroxenite	5% ol ($Fo_{0.930}Fa_{0.070}$), 90% cpx ($Di_{0.700}Hdn_{0.025}Ja_{0.250}En_{0.025}$), 5% grt ($Py_{0.250}Gr_{0.500}Alm_{0.250}$)

Therefore, carbon was set in equilibrium with diamond for the carbonatitic fluid, and the model calculated the most stable mineral assemblage in the system. Finally, to allow the like-for-like comparison with the carbonatitic fluid, we also simulated a suite of peridotitic and eclogitic fluid-rock reactions in equilibrium with diamond (labelled as Type: Diamond in Table 1 and Table S2).

The mineralogy and geochemistry of the reactant rocks are benchmarked to nature using empirical data from natural samples: peridotites (Pearson et al., 2014), eclogites (Pearson et al., 2014; Sverjensky and Huang, 2015) and pyroxenites (Gonzaga et al., 2010; Farré-de-Pablo et al., 2020; Liu et al., 2022; Lu et al., 2022). Three lithologies represent each rock family with different mineral abundances and solid solution compositions (Table 2). The decision to include pyroxenites was taken due to the predicted genetic relationship between diamonds and pyroxenites, as suggested by Kiseeva et al. (2016).

Reaction path calculations output a large amount of data (Supplementary Material, Table S4–S6). The chemistry of fluids and metasomatic minerals is relevant for this study at each reaction stage until the system is fully equilibrated. Reaction progress is quantified using the reaction variable ξ, which expresses the destruction of 1.0 mole of each reactant mineral per 1.0 kg of H_2O in the initial fluid. To compare with natural data, we plotted the model results over a database of lithospheric diamond inclusion geochemistry, including the major element data for olivine (n = 1334), orthopyroxene (n = 446), clinopyroxene (n = 926) and garnet (n = 2628) (Gurney and Boyd, 1982; Gurney et al., 1984; Viljoen et al., 1998; Jacob et al., 2000; Tappert et al., 2005; Stachel and Harris, 2008; De Stefano et al., 2009; Sobolev et al., 2009; Tappert et al., 2009; Bulanova et al., 2010; Dobosi and Kurat, 2010; Miller et al., 2014; Mikhail et al., 2019b). All input and output files are available at https://doi.org/10.17630/9573e741-2787-4d70-b47a-60e567abccf7.

3. Results

The results of the model runs are given in the Supplementary Material, Table S4–S6. This study focuses on the composition of fluid and solid components, including the solid solution geochemistry of each applicable phase and the speciation of aqueous components dissolved in the fluid as a function of reaction progress (ξ). The metasomatic minerals formed after the reaction are silicates (olivine, pyroxenes, garnet, coesite and meionite), oxides (magnetite and hematite), carbonates (dolomite and aragonite), hydroxides (brucite) and native carbon (diamond) (Table S4). Except for minor meionite, the mineral phases precipitated in our models are consistent with those found as inclusions in mantle diamonds (Stachel et al., 2022). Diamond is present in the final mineral assemblage or as an intermediate product in models involving peridotitic and carbonatitic fluids in equilibrium with diamond (initial fluid C-content > 5.00 molal; Table 1). Instead, for eclogitic fluids in equilibrium with diamond where the initial fluid C-content is lower (initial fluid C-content = 3.13 molal; Table 1), diamond does not precipitate. In this work, we term diamond-forming fluids as all the fluids in equilibrium with diamond before the fluid-rock interaction, regardless of their ability to precipitate diamond during the modelled metasomatic reactions. Meionite is formed because the system needs to compensate for the high activities of calcium and carbon in the early stages of the fluid-rock interaction under conditions where carbonates and clinopyroxenes are unstable. As the reaction progresses, meionite is often supplanted by clinopyroxene, carbon-rich aqueous species, and occasionally, diamond. Our models show that the precipitation of metasomatic garnets and clinopyroxenes with chemical compositions covering almost entirely the range of silicate minerals found as inclusions in diamonds is possible during fluid metasomatism of the SCLM. Garnet and clinopyroxene are present in the final stages of every model presented in this work, with some exceptions when a carbonatitic fluid is involved (Table S4). Herein, we focus on the chemical evolution of garnets and clinopyroxene because these phases are present and common in all three paragenetic diamond inclusion groups.

3.1. Reaction products as a function of the fluid type (diamond-forming fluids)

Selected models charting the geochemical evolution of precipitated garnets and clinopyroxenes are shown in Fig. 3. Consistent with the findings for eclogitic fluid-rock metasomatism reported previously (Mikhail et al., 2021), varying the silicate mineral abundances and solid-solution compositions in the host rock does not strongly influence the geochemistry of the precipitates from a given fluid. These data show, as can be expected, that those reactions with the most significant chemical disequilibrium between fluid and rock produce the broadest compositional range of silicate precipitates. For example, model runs for an eclogitic fluid reacting with a lherzolite show a wide variation in garnet and clinopyroxene compositions (Fig. 3c and 3d).

We find the composition of garnets precipitated from both the eclogitic and peridotitic fluids reacting with all mantle lithologies overlaps with natural diamond inclusion data on the pyrope-grossular-almandine ternary, with garnet compositions transecting the fields encompassing high-Mg eclogitic, websteritic, and peridotitic garnet inclusion compositions (Fig. 3a and 3c). The composition of clinopyroxenes precipitated from the peridotitic fluid shows Mg-enrichment and Fe-depletion outside the range observed in the natural diamond inclusion dataset (Fig. 3b). In contrast, the composition of clinopyroxenes precipitated from the eclogitic fluid shows substantial overlap with the natural diamond inclusion dataset in wollastonite-enstatite-ferrosilite space, crossing the field for eclogitic, websteritic, and peridotitic compositions (Fig. 3d).

For the carbonatitic fluid, we find that not all the models predict the precipitation of garnet. When it happens, the garnet produced has hereto unseen, very high, grossular contents because of the elevated Ca-content (dissolved Ca-carbonate) in the system (Fig. 3e) and produce clinopyroxene with appropriate Ca/Mg ratios and severely depleted Fe contents (Fig. 3f). This means that [1] garnets found as inclusions in diamonds may have yet to experience carbonatitic metasomatism, or [2] the geochemistry of the carbonatitic fluids in our model is not a good match for the carbonatitic fluids in nature. As no experimental studies show the primary composition of diamond-forming carbonatitic fluids and fluid inclusions in natural diamonds are not primary (compositionally), the calibration of a carbonatitic fluid through natural or experimental data is not feasible at present. Therefore, we do not consider models involving this carbonatitic fluid furthermore. Still, we provide ternary diagrams showing the results for carbonatitic fluid models in the Supplementary Material (Fig. S1).

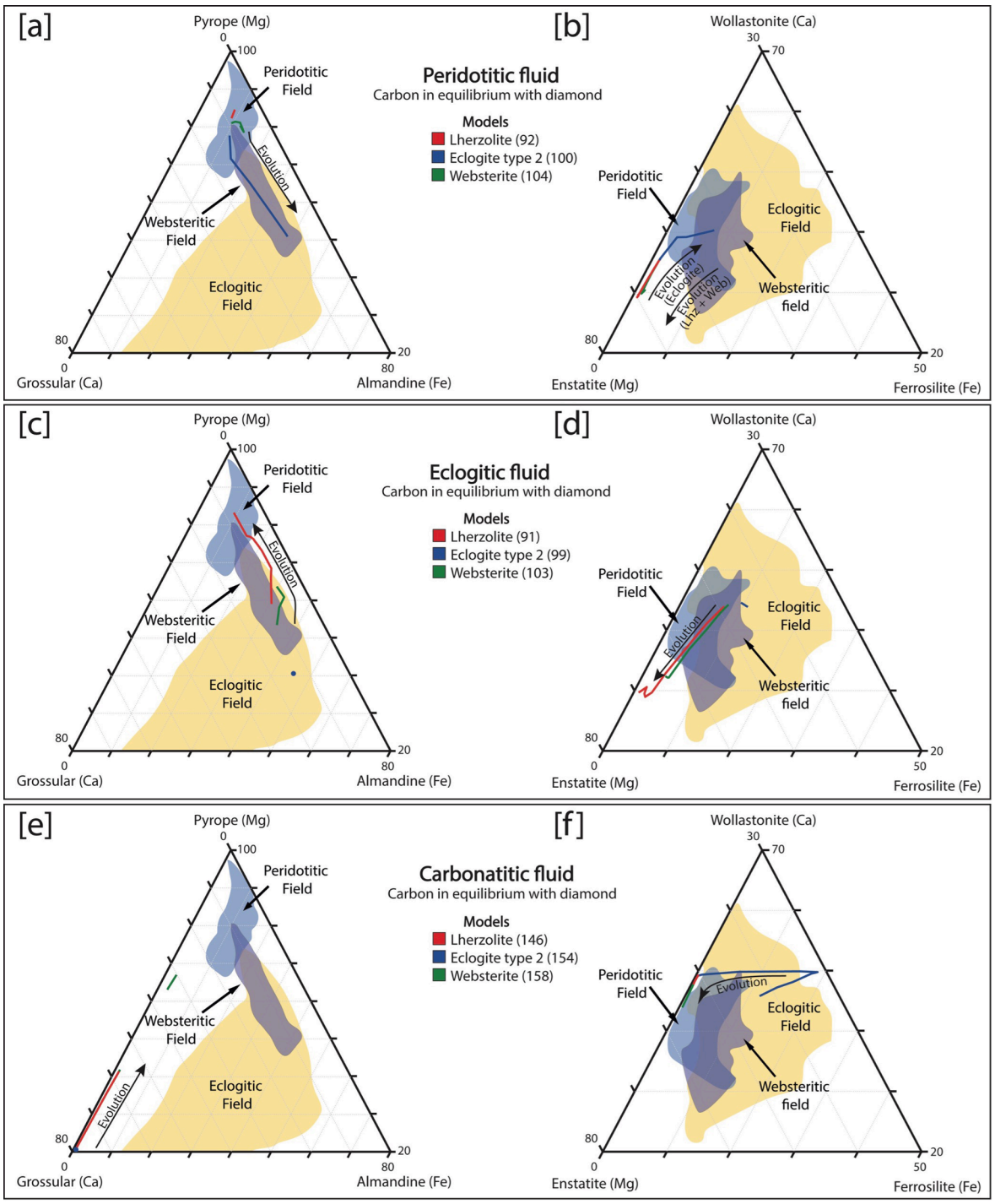

Fig. 3. Geochemistry of garnets and clinopyroxenes precipitated during progressive fluid-rock interaction for peridotitic (a, b), eclogitic (c, d), and carbonatitic (e, f) diamond-forming fluids with a range of host rocks (lherzolite, eclogite type 2, and websterite) at 1000 °C, 5 GPa and $\log fO_2 = -3$ ΔFMQ. The initial amount of carbon in the fluids is determined by equilibrium with diamond (diamond-forming fluids) and varies from about 3 to 18 molal. The numbers in parentheses refer to the model run number.

3.2. Reaction products as a function of the carbon content of the fluid

The trends described above for the model predicted garnet and clinopyroxene compositions consistent with carbon-rich initial fluids (i.e., diamond-forming fluids) serve as reference trends and are reported as black lines in Fig. 4. Among the most abundant dissolved carbon species in these fluids include $Ca(HCOO)^+$, $Fe(HCOO)^+$ and $Mg(SiO_2)(HCO_3)^+$ (Table S3 and Table S6). Therefore, a rational assumption would be that aqueous Mg-Ca-Fe-C complexes will exert control on the behaviour of Mg^{2+}, Ca^{2+} and Fe^{2+}, which would be reflected in the composition of calcium-bearing ferromagnesian silicates. Indeed, we find that the carbon content of the fluid greatly influences the chemical composition of garnets and clinopyroxenes precipitated during fluid-rock interaction. In short, the lower the carbon content in the fluid, the lower the Mg-contents in garnet and clinopyroxene precipitates (Fig. 4a and 4d). For example, it can be seen in Fig. 4a and 4c that model carbon-poor fluids (carbon less than or equal to 1.00 molal) show a very different chemical evolution to the carbon-rich diamond-forming fluid in terms of the

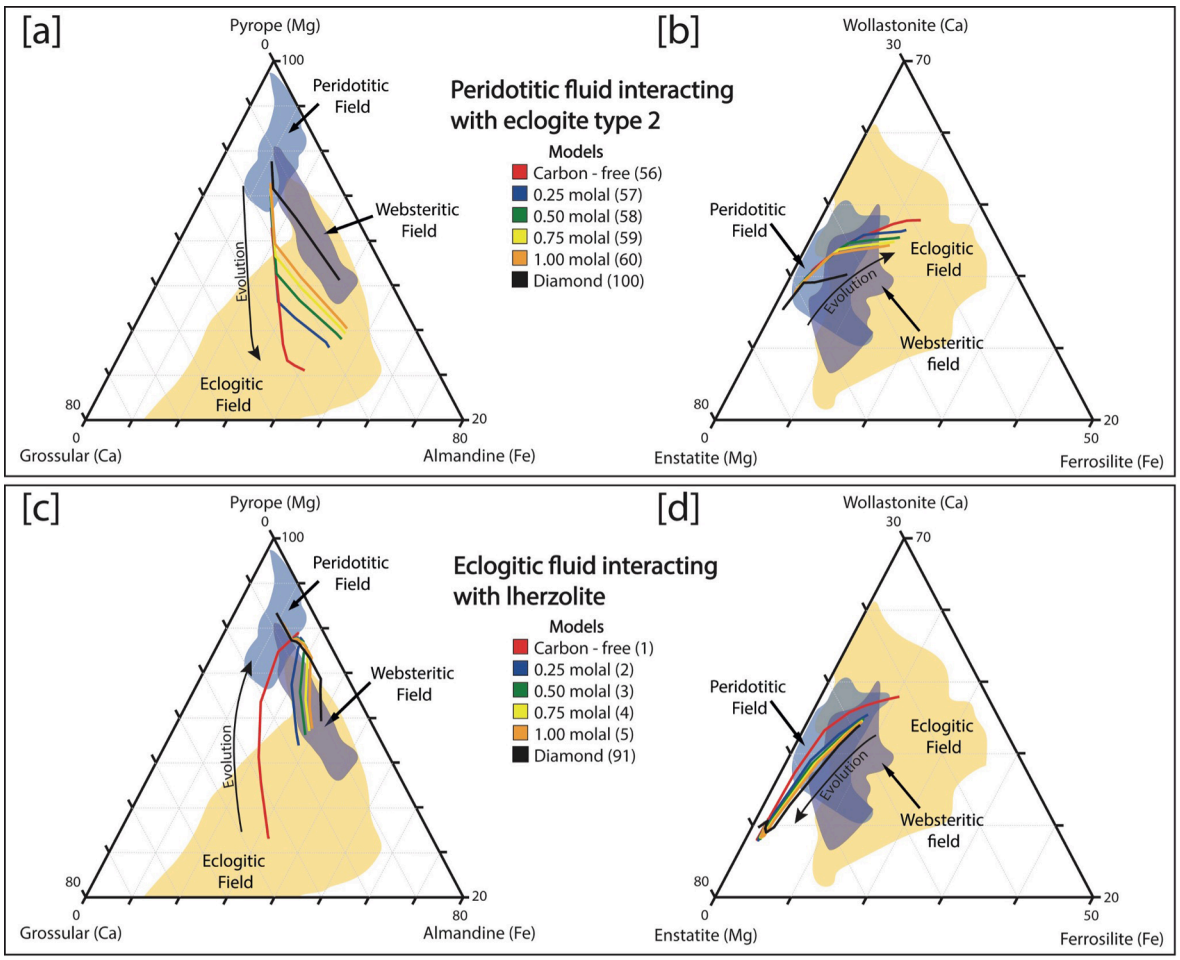

Fig. 4. Results for models with variable carbon contents. Garnet and clinopyroxene chemical compositions resulting from the interaction between peridotitic (a, b) and eclogitic (c, d) fluids with a range of host rocks (lherzolite, eclogite type 2, and websterite) at 1000 °C, 5 GPa and logfO_2 = -3 ΔFMQ. The amount of carbon varies from carbon-free to those in equilibrium with diamond. The numbers in parentheses refer to the model run number.

predicted garnet compositions. In fact, the lowest carbon fluids (C-free) are consistent with garnets with pyrope contents of only 30% (Fig. 4a and 4c). The same fluids are consistent with clinopyroxenes with enstatite contents as low as about 50% and high wollastonite and ferrosilite contents (Fig. 4b and 4d). The range of predicted model clinopyroxene compositions results in model trajectories which cross from the truly eclogitic (Fe-rich + Mg-poor) areas of these ternary diagrams into the Mg-rich and definitively peridotitic domain(s) (Fig. 4b and 4d).

4. Discussion

4.1. Towards a quantitative definition for metasomatic fluids

A silicate melt comprises a liquid with a three-dimensional polymerised network of Si or Si-Al tetrahedrons, but there is no quantitative or empirical definition of a metasomatic fluid. The term *fluid* is widely used in mantle petrology, where the postulated middle ground between fluid and melt is called a hydrous melt. However, there is a continuous solubility curve between SiO_2 (melt) and H_2O (fluid) in the SiO_2-H_2O system (Newton & Manning, 2008), and complete miscibility can occur under the right P-T-X conditions, converting the binary system into a single phase (Bureau & Keppler, 1999). Therefore, the position of a hydrous melt is difficult to define. Effectually then, the term fluid is used to posit a solvent which acts as a mobilising agent where the framework is not polymerised but is thought to be dominated by H_2O above the second critical endpoint (the termination of the solidus in a P-T space; Wyllie & Ryabchikov 2000; Kessel et al., 2005a,b). Weiss et al. (2022) note that – for mantle PT conditions – if a working definition for fluid considers all phases included in diamonds that were *fluid* (i.e., not solid and above the second critical endpoint) at the time of entrapment, then a definition for high-density fluids (HDFs) would include silicate, sulfide, metallic, carbonatitic or saline super-solidus melts and dense hydrous fluids. They place a quantitative division based on density for a C-O-H fluid carrying a few tens of per cent solute where, at lithospheric pressures and temperatures, these low-density fluids would have densities of $\sim$ 1000 kg/m^3 and high-density fluids would be $>$ 2000 kg/m^3, with a continuous transition between low-and high-density fluids. In this study, we do not consider density and adopt a simple geochemical constraint to define our meaning of the term *fluid*. We show that aqueous fluids can contain $>$ 50 mol% solutes at upper mantle pressures, comprising the key rock-forming elements (Na-K-Mg-Ca-Fe-Si-Al) dissolved in the form of aqueous ions, complexes, and neutral species (Fig. 5). Furthermore, the data provided in Fig. 5 clearly highlight that a fluid can be close to 100 mol% H_2O or $<$ 50 mol% H_2O, meaning it is very difficult to intrinsically define the nature of a metasomatic fluid under mantle-like P-T-X conditions, save for stating that the metasomatic agent's framework is not a polymerised network of Si or Si-Al tetrahedrons and is not a liquid carbonate melt. Herein, we adopt a working definition for fluid as a metasomatic agent with at least 40 mol% H_2O (Fig. 5a and 5b).

4.2. Chemical evolution during carbon-bearing fluid-rock interaction

The systems investigated in this study are isobaric and isothermal, where each run has a fixed starting fO_2. We observe minor (and trivial)

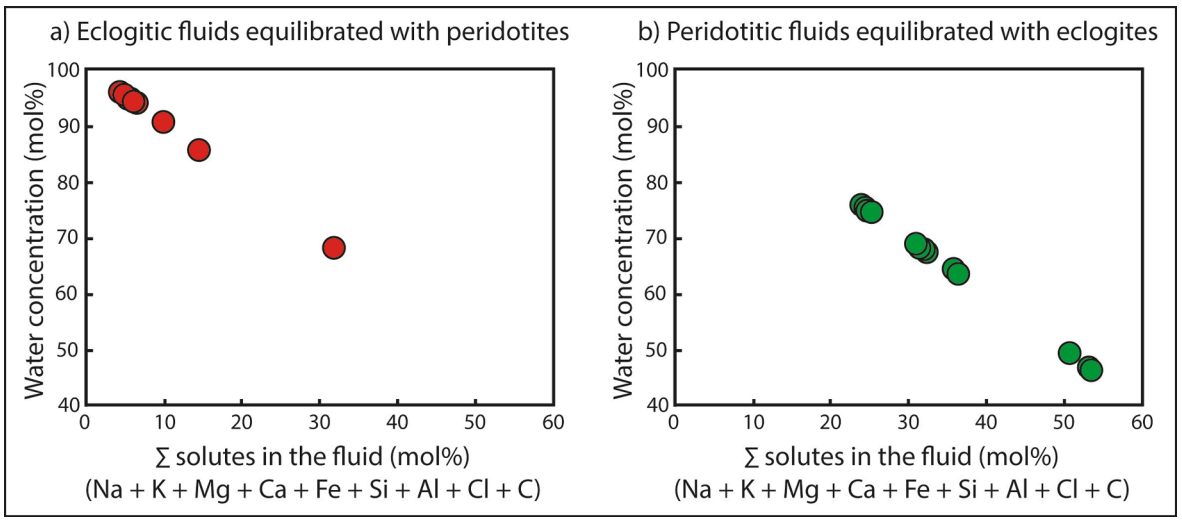

Fig. 5. Example model results showing fluid compositions for [a] eclogitic fluids equilibrated with peridotites and [b] peridotitic fluids equilibrated with eclogites (Table S5). The data provided show that a fluid can be close to 100 mol% H_2O or < 50 mol% H_2O, meaning it is very difficult to intrinsically define the nature of a metasomatic fluid.

variations in oxygen fugacity (in the second decimal place) and pH during each run. Consequently, the driving force for metasomatism is the chemical gradient established between the system's two components, a model rock and a model fluid. Our models predict that fluid-rock interaction will result in progressive silicate formation with evolving major element compositions. Both fluids and rocks play a role in mineral evolution. Counter-intuitively, host rock mineralogy is not always reflected in the geochemistry of the precipitates at each reaction stage. Instead, the geochemistry of the fluid dominates the nature of mineral precipitates in the early stages (low ξ). However, the mineral composition of the precipitates eventually converges with those of the host rock at high ξ. For example, the first garnets and pyroxenes precipitating from an eclogitic fluid reacting with a lherzolite are grossular- and diopside-rich, but the final garnets and clinopyroxenes precipitating at the end of the same reaction pathway are relatively pyrope- and enstatite-rich (Figs. 3c and 4c). Additionally, the clinopyroxenes formed by a peridotitic fluid reaction with a lherzolite and websterite increase their enstatite component when the host rock is more Mg-rich than the peridotite which formed the peridotitic fluid (Fig. 3b).

We use data from lithospheric diamond inclusions (Fig. 1b) as a calibrant for model accuracy. Both eclogitic and peridotitic fluids precipitate garnets that transect (peridotitic fluid; Fig. 4a) or straddle (eclogitic fluid; Fig. 4c) the spread of natural data. Carbon-poor (0.00 to 1.00 molal) fluids do not produce diamond in our models, and the composition of the resulting metasomatic garnets is Ca-rich. In contrast, diamond-forming fluids in our model produce garnet with >50% pyrope. These constraints prevent the prediction of the formation of pyrope-poor eclogitic garnet together with diamond during the same metasomatic events. However, the majority of eclogitic garnet inclusions in diamonds are pyrope-poor (Fig. 1b).

A similar trend is observed for clinopyroxenes, and both peridotitic and eclogitic show substantial overlap with natural data. Diamond-forming fluids precipitate sub-calcic clinopyroxenes (< 45% Wo), while carbon-poor fluids are responsible for higher calcium content (Fig. 4b and 4d).

Whilst far from encompassing the range of garnet and clinopyroxene major element compositions found in lithospheric diamonds, these models corroborate the notion that eclogitic, websteritic, and peridotitic garnet and clinopyroxene inclusions in lithospheric mantle diamonds can be genetically related to one another by a single metasomatic event (Mikhail et al., 2021). We show that this notion holds, non-exclusively, for garnets and clinopyroxenes precipitated during the metasomatic interaction of eclogitic and peridotitic fluid with the main mantle-forming rocks (peridotite, websterite, and eclogite).

Previous experimental studies predict the coexistence of carbonates with native carbon (Poli et al., 2009; Foley et al., 2009; Dasgupta and Hirschmann, 2010; Poli, 2015), whereas our models do not predict abundant carbonate precipitation. In models involving carbonatitic fluids, carbonates (dolomite and aragonite) are mostly intermediate products (Fig. S3a). Instead, diamond is the most stable solid carbon phase at the investigated P-T-X-fO_2 conditions. However, some of our models predict carbonate in the final metasomatic assemblage at logfO_2 = −2 ΔFMQ (Table S4), and their compositions match the experimental data (Fig. S3b). Two reasons can be addressed: [1] the systems in this study are too reduced to stabilise carbonate minerals (logfO_2 ≤ 0 ΔFMQ), and [2] the systems are carbon undersaturated. Therefore, if we increased the carbon content of the fluid or the oxygen fugacity of the system, we would force the precipitation of carbonates instead of native carbon. Nevertheless, forming solid carbon phases is not the objective of this study, as we focus on the range of garnet and clinopyroxene compositions produced during fluid-rock metasomatism.

4.3. *Chemical evolution during carbon-poor fluid-rock interaction*

Any individual diamond-hosted mineral inclusion is either syngenetic (Harris, 1968; Mikhail et al., 2019b) or protogenetic (Nestola et al., 2017; Pasqualetto et al., 2022) to the host diamond. If syngenetic, the formation of inclusions in diamonds is the result of carbon-rich fluid metasomatism, according to our models. Our data imply that diamond-forming fluids cannot produce pyrope-poor garnets and wollastonite + ferrosillite -rich clinopyroxenes under the conditions employed in this study. This may suggest that pyrope-poor garnet and wollastonite + ferrosillite -rich clinopyroxene inclusions are protogenetic, and their geochemistry should reflect their protolith (eclogite). Alternatively, they may reflect a previous metasomatic event before being incorporated into diamond. In both cases, the inclusions can be thought of as protogenetic, and these samples would be incredibly valuable tracers of metasomatism, mantle melting, and subduction events through deep time.

Our models predict that the amount of carbon strongly influences the major element composition of garnets and clinopyroxenes precipitated from the fluid. As indicated above, most carbon-poor fluids form Mg-poor and Ca-rich garnets (Fig. 4a and 4c) and clinopyroxenes (Fig. 4b and 4d). Metasomatic reactions for both carbon-poor peridotitic fluids (Fig. 4a and 4b) and carbon-poor eclogitic fluids (Fig. 4c and 4d) result

in the precipitation of garnets and clinopyroxenes deep in the eclogitic field of data, where Ca-rich phases dominate. In contrast, carbon-rich fluids initially in equilibrium with diamond resulted in Mg-rich garnets (Fig. 3a and 3c) and clinopyroxenes (Fig. 3b and 3d), covering the whole range of peridotitic and websteritic inclusions but barely entering the low-Mg eclogitic field.

As anticipated, we attribute the effects of variable carbon concentration on the silicate product minerals to the speciation of bivalent ions as Mg-Ca-Fe-C aqueous complexes during the metasomatic process. The model Mg-rich aqueous species are more abundant in the more-oxidized carbon-rich systems, consistent with experimental data (Tiraboschi et al., 2018). Evidence for the role of oxygen fugacity on the aqueous speciation is found by examining the effect of different oxygen fugacities ($\log fO_2 = -2$ to -4 ΔFMQ) on the composition of silicate precipitates during the fluid-rock interaction (Fig. S2). The amount of carbon in the fluid and its speciation are susceptible to variations in the redox conditions (Table 1, Table S2–S3). By lowering the oxygen fugacity, the total Mg/total C ratio decreases because of the differences in the Mg-silicate-bicarbonate and Ca-formate aqueous complexes. This means a proportional higher availability of Ca-formate complexes, leading to the formation of Ca-rich silicates, which cross deeper into the eclogitic field.

4.4. *Implications for diamond-inclusion petrogenesis*

Carbon speciation does not solely control silicate composition, it is also linked to the formation of diamond. However, diamond is not formed in the carbon-undersaturated models in this study (Table S4). In our models, Mg-poor garnets and clinopyroxenes form from low-carbon fluid metasomatism. Therefore, these data imply that Mg-poor eclogitic diamond inclusion did not form during the metasomatic event which formed their host diamond. These inclusions are, therefore, likely protogenetic. Thus, their geochemistry should strongly reflect an eclogite protolith or, alternatively, a metasomatic event prior to the formation of the host diamond. Conversely, our data also show that carbon-rich fluid metasomatism results in the formation of Mg-rich garnets and clinopyroxenes. This result implies that peridotitic and websteritic garnets and clinopyroxenes can be either syngenetic or protogenetic.

Testing our models is challenging due to a dearth of data from natural samples and/or high-pressure experiments. Therefore, we compare our model trajectories with the scarce data available. These are [1] a unique sample extracted from the Jericho kimberlite (NW Slave Craton, Canada; Kopylova and Hayman, 2008) and [2] a recent set of experiments designed to simulate hydrous melt metasomatism in the SCLM (Pintér et al., 2022). Firstly, as with most kimberlites, Jericho provides a suite of mantle xenoliths spanning a wide range of lithologies (eclogite, coarse and deformed peridotite, megacrystalline websterite and ilmenite-garnet wehrlite; Kopylova et al. 1999). Among these, there is a sample of diamondiferous eclogite which has generated a unique dataset: the geochemistry of garnets from diamond inclusions and the geochemistry of garnets from a certified host rock (Smart et al., 2012). These data indicate that diamond-hosted garnets in a single xenolith can show major element heterogeneity between individual diamonds in the

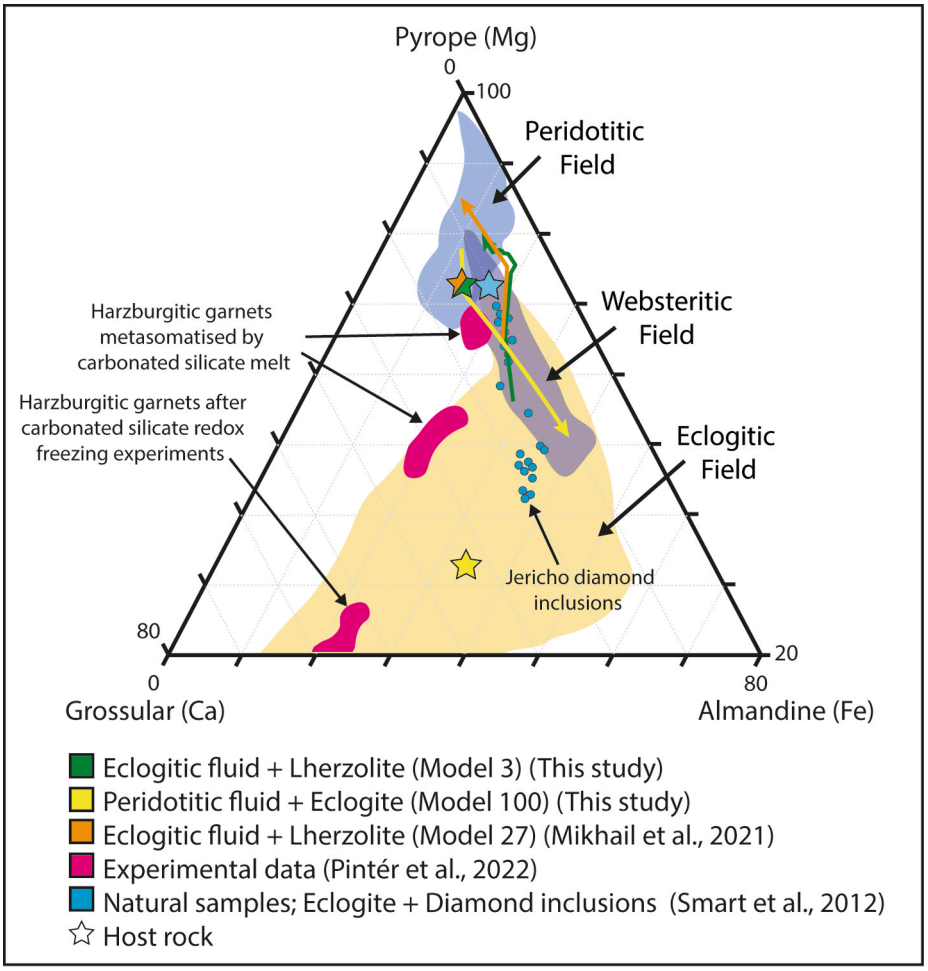

Fig. 6. Garnet compositions from a) natural samples from Jericho (Canada) where the diamond inclusions show different garnet compositions (small blue points) to their host eclogite (large blue star; Smart et al., 2012), b) experiments simulating the interaction between hydrous carbonated silicate melts and harzburgite (fuchsia fields; Pintér et al., 2022), and c) theoretical simulations of fluid-rock metasomatism (orange, yellow, and green arrows and stars; Mikhail et al., 2021 and this study).

same source rock and be all distinct from their host eclogite (Fig. 6). Secondly, Pintér et al. (2022) simulated the interaction between hydrous carbonated silicate melts and harzburgite, and the resulting geochemistry of their metasomatic garnets (Fig. 6). These comparisons show that our model trajectories are coherent with natural data from Jericho diamond inclusions, where the interaction between a high-MgO eclogite and a carbonated melt/fluid is responsible for a broad range of websteritic and eclogitic garnets (Smart et al., 2012). The experimental garnets are more grossular-rich than our model garnets, but they do show the same directional compositional trend, with an evolution towards more Mg-rich endmembers during metasomatism (Fig. 6). Therefore, these comparative datasets prove that a single metasomatic event can form silicates with different chemical compositions, and these minerals mostly reflect the elemental composition of the fluid/melt instead of the geochemistry of the host rock. Therefore, the paragenetic groups used to classify diamonds (Stachel and Harris, 2008) should not be considered a genetic classification, as the role of the fluid/melt appears to be more relevant than the one played by the host rock.

5. Conclusions

We modelled the interaction between three fluids found as diamond inclusions (peridotitic, eclogitic and carbonatitic) with a broad range of mantle rocks (peridotites, eclogites and pyroxenites) at conditions relevant to the diamond formation (1000 °C, 5 GPa, −2 to −4 ΔFMQ) to simulate fluid-rock metasomatism. We specifically focused on a wide range of initial carbon concentrations in the metasomatic fluids to explore the effects on the chemical evolution of garnets and clinopyroxenes during metasomatic processes. We studied how different fluids, rocks, amounts of carbon, and environmental conditions can influence the major element composition of silicate inclusions in diamonds.

Our results show that the driving force for silicate evolution is the chemical gradient established between the host rock and the fluid, leading to the possibility of connecting different paragenetic groups along a single reaction pathway in an isobaric and isothermal system. In our models, both fluids and host rocks play an important role in controlling the silicate chemical evolution: the fluid is responsible for the initial composition of metasomatic minerals, and later, when the magnitude of fluid-rock interaction increases, the host rock becomes dominant. These data highlight how paragenetic groups of inclusions from diamonds are not necessarily directly related to a particular geological environment in every case. Instead, the traditional paragenetic groups can reflect the extent of the metasomatic process and the nature of the original metasomatic fluid.

Importantly, the amount of carbon in the initial fluid strongly influences the composition of silicate minerals formed during metasomatism. Carbon-poor fluids are necessary to form Mg-poor, Ca-rich garnets and clinopyroxenes, but do not form diamond under the conditions we examined. This result suggests that a syngenetic origin of diamonds and low-Mg eclogitic inclusions may not be feasible during the same metasomatic event. Such inclusions in diamonds may well be protogenetic. In contrast, carbon-rich fluids can precipitate Mg-rich minerals and diamond. Therefore, peridotitic and websteritic inclusions in diamonds can be either syngenetic or protogenetic, and no single notion can be championed beyond a reasonable doubt without direct evidence from the sample(s) in question. We suggest that focus should be directed towards diamonds containing multiple inclusions of the same mineral group (especially garnets and clinopyroxenes), where each inclusion is examined for its crystallographic orientation, major and trace element geochemistry, and relative geochronology.

Declaration of Competing Interest

The authors declare that they have no known competing financial interests or personal relationships that could have appeared to influence the work reported in this paper.

Data availability

Data are available through PURE (St Andrews University repository system) at https://doi.org/10.17630/9573e741-2787-4d70-b47a-60e567abccf7.

Acknowledgements

We are grateful to Thomas Stachel for sharing their extensive database for mineral inclusions in diamonds, without which this study would have taken several years to complete. MR, SM and JK acknowledge support from NERC standard grant (NE/PO12167/1) and UK space agency Aurora grant (ST/T001763/1). DAS acknowledges support from NSF Grant #2032039 and DOE Grant #DE-SC0019830. SM is grateful to Oded Navon and Hugh O'Neill for enjoyable and insightful discussions concerning how mantle fluids are (and are not) defined. We are grateful for the constructive peer review process handled by Prof Rajdeep Dasgupta and provided by Prof Stefano Poli and another anonymous reviewer, which improved the clarity of this contribution.

Appendix A. Supplementary material

The Supplementary Material contains the composition and carbon speciation of the fluids before and after the fluid-rock interactions, and the final rock composition for the most relevant models. Ternary plots for different rocks and variations in oxygen fugacity are also available. Supplementary Material to this article can be found online at https://doi.org/10.1016/j.gca.2023.06.025.

References

Aulbach, S., Stachel, T., Creaser, R.A., Heaman, L.M., Shirey, S.B., Muehlenbachs, K., Eichenberg, D., Harris, J. W., 2008. Sulfide survival and diamond genesis during formation and evolution of Archaean subcontinental lithosphere: Slave vs Kaapvaal. International Kimberlite Conference: Extended Abstracts 9.

Aulbach, S., Stachel, T., Viljoen, K.S., Brey, G.P., Harris, J.W., 2002. Eclogitic and websteritic diamond sources beneath the Limpopo Belt - Is slab-melting the link? Contrib. Mineral. Petrol. 143, 56–70.

Bulanova, G.P., Walter, M.J., Smith, C.B., Kohn, S.C., Armstrong, L.S., Blundy, J., Gobbo, L., 2010. Mineral inclusions in sublithospheric diamonds from Collier 4 kimberlite pipe, Juina, Brazil: Subducted protoliths, carbonated melts and primary kimberlite magmatism. Contrib. Mineral. Petrol. 160, 489–510.

Bureau, H., Keppler, H., 1999. Complete miscibility between silicate melts and hydrous fluids in the upper mantle: experimental evidence and geochemical implications. Earth. Planet. Sci. Lett. 165, 187–196.

Bureau, H., Remusat, L., Esteve, I., Pinti, D.L., Cartigny, P., 2018. The growth of lithospheric diamonds. Sci. Adv. 4, eaat1602.

Dasgupta, R., Hirschmann, M.M., 2010. The deep carbon cycle and melting in Earth's interior. Earth. Planet. Sci. Lett. 298, 1–13.

De Stefano, A., Kopylova, M.G., Cartigny, P., Afanasiev, V., 2009. Diamonds and eclogites of the Jericho kimberlite (Northern Canada). Contrib. Mineral. Petrol. 158, 295–315.

Dobosi, G., Kurat, G., 2010. On the origin of silicate-bearing diamondites. Mineral. Petrol. 99, 29–42.

Facq, S., Daniel, I., Montagnac, G., Cardon, H., Sverjensky, D.A., 2014. In situ Raman study and thermodynamic model of aqueous carbonate speciation in equilibrium with aragonite under subduction zone conditions. Geochim. Cosmochim. Acta 132, 375–390.

Farré-de-Pablo, J., Pujol-Solà, N., Torres-Herrera, H., Aiglsperger, T., González-Jiménez, J.M., Llanes-Castro, A.I., Garcia-Casco, A., Proenza, J.A., 2020. Orthopyroxenite hosted chromitite veins anomalously enriched in platinum-group minerals from the Havana-Matanzas Ophiolite, Cuba Vetas de cromitita en ortopiroxenita anómalamente enriquecidas en minerales del grupo del platino de la ofiolita Habana-Matanzas, Cuba. Boletin de la Sociedad Geologica Mexicana 72, 1–22.

Foley, S.F., Yaxley, G.M., Rosenthal, A., Buhre, S., Kiseeva, E.S., Rapp, R.P., Jacob, D.E., 2009. The composition of near-solidus melts of peridotite in the presence of CO_2 and H_2O between 40 and 60 kbar. Lithos 112, 274–283.

Förster, M.W., Foley, S.F., Marschall, H.R., Alard, O., Buhre, S., 2019. Melting of sediments in the deep mantle produces saline fluid inclusions in diamonds. Sci. Adv. 5, eaau2620.

Gonzaga, R.G., Lowry, D., Jacob, D.E., LeRoex, A., Schulze, D., Menzies, M.A., 2010. Eclogites and garnet pyroxenites: Similarities and differences. J. Vol. Geotherm. Res. 190, 235–247.

Gress, M.U., Koornneef, J.M., Thomassot, E., Chinn, I.L., van Zuilen, K., Davies, G.R., 2021. Sm-Nd isochron ages coupled with C-N isotope data of eclogitic diamonds from Jwaneng, Botswana. Geochim. Cosmochim. Acta 293, 1–17.

Gurney, J.J., Boyd, F.R., 1982. Mineral intergrowths with polycrystalline diamonds from Orapa Mine, Botswana. Carnegie Instit. Wash. Year 81, 267–273.
Gurney, J.J., Harris, J.W., Rickard, R.S., 1984. Silicate and Oxide Inclusions in Diamonds from the Orapa Mine, Botswana. Kimberlites II: Mantle Crust-Mantle Relationships 11, 3–9.
Gurney, J.J., Helmstaedt, H.H., Richardson, S.H., Shirey, S.B., 2010. Diamonds through Time. Econ. Geol. 105, 689–712.
Hao, J., Sverjensky, D.A., Hazen, R.M., 2016. A model for late Archean chemical weathering and world average river water. Earth Planet. Sci. Lett. 457, 191–203.
Hao, J., Sverjensky, D.A., Hazen, R.M., 2017. Mobility of nutrients and trace metals during weathering in the late Archean. Earth Planet. Sci. Lett. 471, 148–159.
Harris, J., 1968. The recognition of diamond inclusions. Part 1: syngenetic mineral inclusions. Ind. Diamond Rev. 28, 402–410.
Helgeson, H.C., Kirkham, D.H., 1974a. Theoretical prediction of the thermodynamic behavior of aqueous electrolytes at high pressures and temperatures; I, Summary of the thermodynamic/electrostatic properties of the solvent. Am. J. Sci. 274, 1089–1198.
Helgeson, H.C., Kirkham, D.H., 1974b. Theoretical prediction of the thermodynamic behavior of aqueous electrolytes at high pressures and temperatures; II, Debye-Huckel parameters for activity coefficients and relative partial molal properties. Am. J. Sci. 274, 1199–1261.
Helgeson, H.C., Kirkham, D.H., 1976. Theoretical prediction of the thermodynamic propertiesof aqueous electrolytes at high pressures and temperatures. III. Equation of state foraqueous species at infinite dilution. Am. J. Sci. 276, 97–240.
Helgeson, H.C., 1979. Mass transfer among minerals and hydrothermal solutions. Geochemistry of Hydrothermal Ore Deposits. H.L. Barnes, Holt, Rhinehart, and Winston, 568–610.
Helgeson, H.C., Kirkham, D.H., Flowers, G.C., 1981. Theoretical prediction of the thermodynamic behavior of aqueous electrolytes by high pressures and temperatures; IV, Calculation of activity coefficients, osmotic coefficients, and apparent molal and standard and relative partial molal properties to 600 degrees C and 5kb. Am. J. Sci. 281, 1249–1516.
Huang, F., Sverjensky, D.A., 2019. Extended Deep Earth Water Model for predicting major element mantle metasomatism. Geochim. Cosmochim. Acta 254, 192–230.
Huang, F., Sverjensky, D.A., 2020. Mixing of carbonatitic into saline fluid during panda diamond formation. Geochim. Cosmochim. Acta 284, 1–20.
Izraeli, E.S., Harris, J.W., Navon, O., 2001. Brine inclusions in diamonds: a new upper mantle fluid. Earth. Planet. Sci. Lett. 187, 323–332.
Jacob, D.E., Viljoen, K.S., Grassineau, N., Jagoutz, E., 2000. Remobilization in the cratonic lithosphere recorded in polycrystalline diamond. Science 289, 1182–1185.
Jacob, D.E., Dobrzhinetskaya, L., Wirth, R., 2014. New insight into polycrystalline diamond genesis from modern nanoanalytical techniques. Earth. Sci. Rev. 136, 21–35.
Kessel, R., Schmidt, M.W., Ulmer, P., Pettke, T., 2005a. Trace element signature of subduction-zone fluids, melts and supercritical liquids at 120–180 km depth. Nature 437, 724–727.
Kessel, R., Ulmer, P., Pettke, T., Schmidt, M.W., Thompson, A.B., 2005b. The water–basalt system at 4 to 6 GPa: Phase relations and second critical endpoint in a K-free eclogite at 700 to 1400 °C. Earth. Planet. Sci. Lett. 237, 873–892.
Kessel, R., Pettke, T., Fumagalli, P., 2015. Melting of metasomatized peridotite at 4–6 GPa and up to 1200 °C: an experimental approach. Contrib. Mineral. Petrol. 169, 1–19.
Kiseeva, E.S., Wood, B.J., Ghosh, S., Stachel, T., 2016. The pyroxenite-diamond connection. Geochem. Perspect. Lett. 2, 1–9.
Koornneef, J.M., Gress, M.U., Chinn, I.L., Jelsma, H.A., Harris, J.W., Davies, G.R., 2017. Archaean and Proterozoic diamond growth from contrasting styles of large-scale magmatism. Nat. Commun. 8, 648.
Kopylova, M.G., Hayman, P., 2008. Petrology and textural classification of the Jericho kimberlite, northern Slave Province, Nunavut, Canada. Can. J. Earth. Sci. 45, 701–723.
Kopylova, M.G., Russell, J.K., Cookenboo, H., 1999. Petrology of peridotite and pyroxenite xenoliths from the Jericho Kimberlite: Implications for the thermal state of the mantle beneath the Slave Craton, Northern Canada. J. Petrol. 40, 79–104.
Leong, J.A., Howells, A.E., Robinson, K.J., Cox, A., Debes, R.V., Fecteau, K., Prapaipong, P., Shock, E., 2021. Theoretical predictions versus environmental observations on serpentinization fluids: Lessons from the Samail ophiolite in Oman. J. Geophys. Res. Solid Earth 126 e2020JB020756.
Leong, J.A.M., Shock, E.L., 2020. Thermodynamic constraints on the geochemistry of low-temperature, continental, serpentinization-generated fluids. Am. J. Sci. 320, 185–235.
Liu, J., Wang, J., Hattori, K., Wang, Z., 2022. Petrogenesis of garnet clinopyroxenite and associated dunite in hujialin, Sulu orogenic belt, Eastern China. Minerals 12, 162.
Lu, J.G., Griffin, W.L., Huang, J.X., Dai, H.K., Castillo-Oliver, M., O'Reilly, S.Y., 2022. Structure and composition of the lithosphere beneath Mount Carmel, North Israel. Contrib. Mineral. Petrol. 177, 1–16.
Luth, R.W., Stachel, T., 2014. The buffering capacity of lithospheric mantle: implications for diamond formation. Contrib. Mineral. Petrol. 168, 1–12.
Manning, C.E., 2013. Thermodynamic modeling of fluid-rock interaction at mid-crustal to upper-mantle conditions. Rev. Mineral. Geochem. 76, 135–164.
McCollom, T.M., Shock, E.L., 1998. Fluid-rock interactions in the lower oceanic crust: Thermodynamic models of hydrothermal alteration. J. Geophys. Res. 103, 547–575.
Meltzer, A., Kessel, R., 2022. The interaction of slab-derived silicic fluid and harzburgite – Metasomatism in the sub cratonic lithospheric mantle. Geochim. Cosmochim. Acta 328, 103–119.
Mikhail, S., Crosby, J.C., Stuart, F.M., DiNicola, L., Abernethy, F.A.J., 2019a. A secretive mechanical exchange between mantle and crustal volatiles revealed by helium isotopes in 13C-depleted diamonds. Geochem. Perspect. Lett. 11, 39–43.
Mikhail, S., McCubbin, F.M., Jenner, F.E., Shirey, S.B., Rumble, D., Bowden, R., 2019b. Diamondites: evidence for a distinct tectono-thermal diamond-forming event beneath the Kaapvaal craton. Contrib. Mineral. Petrol. 174, 1–15.
Mikhail, S., Rinaldi, M., Mare, E.R., Sverjensky, D.A., 2021. A genetic metasomatic link between eclogitic and peridotitic diamond inclusions. Geochem. Perspect. Lett. 17, 33–38.
Miller, C.E., Kopylova, M., Smith, E., 2014. Mineral inclusions in fibrous diamonds: Constraints on cratonic mantle refertilization and diamond formation. Mineral. Petrol. 108, 317–331.
Navon, O., Hutcheon, I.D., Rossman, G.R., Wasserburg, G.J., 1988. Mantle-derived fluids in diamond micro-inclusions. Nature 335, 784–789.
Nestola, F., Jung, H., Taylor, L.A., 2017. Mineral inclusions in diamonds may be synchronous but not syngenetic. Nat. Commun. 8, 14168.
Newton, R.C., Manning, C.E., 2008. Thermodynamics of SiO_2–H_2O fluid near the upper critical end point from quartz solubility measurements at 10 kbar. Earth. Planet. Sci. Lett. 274, 241–249.
Palyanov, Y.N., Kupriyanov, I.N., Khokhryakov, A.F., Ralchenko, V.G., 2015. Crystal growth of diamond. Handbook of crystal growth: bulk crystal growth. Second Ed. 2, 671–713.
Pan, D., Spanu, L., Harrison, B., Sverjensky, D.A., Galli, G., 2013. Dielectric properties of water under extreme conditions and transport of carbonates in the deep Earth. Proc. Natl. Acad. Sci. USA 110, 6646–6650.
Pasqualetto, L., Nestola, F., Jacob, D.E., Pamato, M.G., Oliveira, B., Perritt, S., Chinn, I., Nimis, P., Milani, S., Harris, J.W., 2022. Protogenetic clinopyroxene inclusions in diamond and Nd diffusion modeling—Implications for diamond dating. Geology 50, 1038–1042.
Pearson, D.G., Canil, D., Shirey, S.B., 2014. Mantle Samples Included in Volcanic Rocks: Xenoliths and Diamonds. Treatise Geochem. Second Ed. 3, 169–253.
Pintér, Z., Foley, S.F., Yaxley, G.M., 2022. Diamonds, dunites, and metasomatic rocks formed by melt/rock reaction in craton roots. Commun. Earth Environ. 3, 1–8.
Poli, S., 2015. Carbon mobilized at shallow depths in subduction zones by carbonatitic liquids. Nat. Geosci. 8, 633–636.
Poli, S., Franzolin, E., Fumagalli, P., Crottini, A., 2009. The transport of carbon and hydrogen in subducted oceanic crust: An experimental study to 5 GPa. Earth. Planet. Sci. Lett. 278, 350–360.
Shirey, S.B., Cartigny, P., Frost, D.J., Keshav, S., Nestola, F., Nimis, P., Pearson, D.G., Sobolev, N.V., Walter, M.J., 2013. Diamonds and the geology of mantle carbon. Rev. Mineral. Geochem. 75, 355–421.
Shock, E.L., Canovas, P., 2010. The potential for abiotic organic synthesis and biosynthesis at seafloor hydrothermal systems. Geofluids 10, 161–192.
Shock, E.L., Helgeson, H.C., 1988. Calculation of the thermodynamic and transport properties of aqueous species at high pressures and temperatures: Correlation algorithms for ionic species and equation of state predictions to 5 kb and 1000°C. Geochim. Cosmochim. Acta 52, 2009–2036.
Smart, K.A., Chacko, T., Stachel, T., Tappe, S., Stern, R.A., Ickert, R.B., 2012. Eclogite formation beneath the northern Slave craton constrained by diamond inclusions: Oceanic lithosphere origin without a crustal signature. Earth. Planet. Sci. Lett. 319–320, 165–177.
Sobolev, N.V., Logvinova, A.M., Zedgenizov, D.A., Pokhilenko, N.P., Malygina, E.V., Kuzmin, D.V., Sobolev, A.V., 2009. Petrogenetic significance of minor elements in olivines from diamonds and peridotite xenoliths from kimberlites of Yakutia. Lithos 112, 701–713.
Sonin, V., Tomilenko, A., Zhimulev, E., Bul'bak, T., Chepurov, A., Babich, Y., Logvinova, A., Timina, T., Chepurov, A., 2022. The composition of the fluid phase in inclusions in synthetic HPHT diamonds grown in system Fe–Ni–Ti–C. Sci. Rep. 12, 1–9.
Stachel, T., Harris, J.W., 2008. The origin of cratonic diamonds — Constraints from mineral inclusions. Ore Geol. Rev. 34, 5–32.
Stachel, T., Cartigny, P., Chacko, T., Pearson, D.G., 2022. Carbon and nitrogen in mantle-derived diamonds. Rev. Mineral. Geochem. 88, 809–875.
Stachel, T., Luth, R.W., 2015. Diamond formation — Where, when and how? Lithos 220–223, 200–220.
Stagno, V., Frost, D.J., McCammon, C.A., Mohseni, H., Fei, Y., 2015. The oxygen fugacity at which graphite or diamond forms from carbonate-bearing melts in eclogitic rocks. Contrib. Mineral. Petrol. 169, 1–18.
Sverjensky, D.A., 1984. Oil-field brines as ore-forming solutions. Econ. Geol. 79, 23–37.
Sverjensky, D.A., 1987. The role of migrating oil-field brines in the formation of sediment-hosted Cu-rich deposits. Econ. Geol. 82, 1130–1141.
Sverjensky, D.A., Shock, E.L., Helgeson, H.C., 1997. Prediction of the thermodynamic properties of aqueous metal complexes to 1000°C and 5 kb. Geochim. Cosmochim. Acta 61, 1359–1412.
Sverjensky, D.A., Harrison, B., Azzolini, D., 2014. Water in the deep Earth: The dielectric constant and the solubilities of quartz and corundum to 60 kb and 1200 °C. Geochim. Cosmochim. Acta 129, 125–145.
Sverjensky, D.A., Huang, F., 2015. Diamond formation due to a pH drop during fluid-rock interactions. Nat. Commun. 6, 8702.
Tanger, J.C., Helgeson, H.C., 1988. Calculation of the thermodynamic and transport properties of aqueous species at high pressures and temperatures; revised equations of state for the standard partial molal properties of ions and electrolytes. Am. J. Sci. 288, 19–98.
Tappert, R., Stachel, T., Harris, J.W., Shimizu, N., Brey, G.P., 2005. Mineral inclusions in diamonds from the Panda kimberlite, Slave Province, Canada. Eur. J. Mineral. 17, 423–440.

Tappert, R., Foden, J., Stachel, T., Muehlenbachs, K., Tappert, M., Wills, K., 2009. The diamonds of South Australia. Lithos 112, 806–821.
Timmerman, S., Spivak, A.V., Jones, A.P., 2021. Carbonatitic melts and their role in diamond formation in the deep Earth. Elements 17, 321–326.
Tiraboschi, C., Tumiati, S., Sverjensky, D.A., Pettke, T., Ulmer, P., Poli, S., 2018. Experimental determination of magnesia and silica solubilities in graphite-saturated and redox-buffered high-pressure COH fluids in equilibrium with forsterite + enstatite and magnesite + enstatite. Contrib. Mineral. Petrol. 173, 1–17.
Tomlinson, E.L., Jones, A.P., Harris, J.W., 2006. Co-existing fluid and silicate inclusions in mantle diamond. Earth. Planet. Sci. Lett. 250, 581–595.
Tumiati, S., Tiraboschi, C., Sverjensky, D.A., Pettke, T., Recchia, S., Ulmer, P., Miozzi, F., Poli, S., 2017. Silicate dissolution boosts the CO_2 concentrations in subduction fluids. Nat. Commun. 8, 1–11.
Viljoen, K.S., Phillips, D., Harris, J.W., Robinson, D.N., 1998. Mineral inclusions in diamonds from the Venetia kimberlites, Northern Province, South Africa. In: International Kimberlite Conference: Extended Abstracts, vol. 7, pp. 943–945.
Weiss, Y., Kessel, R., Griffin, W.L., Kiflawi, I., Klein-BenDavid, O., Bell, D.R., Harris, J.W., Navon, O., 2009. A new model for the evolution of diamond-forming fluids: Evidence from microinclusion-bearing diamonds from Kankan, Guinea. Lithos 112, 660–674.
Weiss, Y., Kiflawi, I., Davies, N., Navon, O., 2014. High-density fluids and the growth of monocrystalline diamonds. Geochim. Cosmochim. Acta 141, 145–159.
Weiss, Y., McNeill, J., Pearson, D.G., Nowell, G.M., Ottley, C.J., 2015. Highly saline fluids from a subducting slab as the source for fluid-rich diamonds. Nature 524, 339–342.
Weiss, Y., Czas, J., Navon, O., 2022. Fluid inclusions in fibrous diamonds. Rev. Mineral. Geochem. 88, 475–532.
Wyllie, P.J., Ryabchikov, I.D., 2000. Volatile components, magmas, and critical fluids in upwelling mantle. J. Petrol. 41, 1195–1206.
Yaxley, G.M., Kjarsgaard, B.A., Jaques, A.L., 2021. Evolution of carbonatite magmas in the upper mantle and crust. Elements 17, 315–320.